

# An *ab initio* investigation of spin-allowed and spin-forbidden pathways of the gas phase reactions of $O(^3P) + C_2H_5I$

Jonathan E. Stevens, Qiang Cui, and Keiji Morokuma

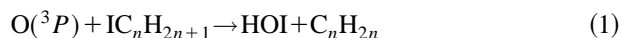
Cherry L. Emerson Center for Scientific Computation and Department of Chemistry, Emory University, Atlanta, Georgia 30322

(Received 1 August 1997; accepted 7 October 1997)

The singlet and triplet potential energy surfaces involved in the gas phase reactive collisions of  $O(^3P)$  and  $C_2H_5I$  have been studied with *ab initio* electronic structure computations. The collisions produce both spin-forbidden  $HOI + C_2H_4$  and spin-allowed  $OI + C_2H_5$  products. The calculations indicate that  $HOI$  is formed via a triplet complex and through a triplet/singlet intersystem crossing, followed by passage through a singlet intermediate and transition state for the intramolecular abstraction of  $\beta$ -hydrogen. All the relevant structures for this pathway are lower in energy than the reactants, and this pathway is accessible even at low impact energies. The calculations also indicate that  $OI$  may be formed by two channels. One is the same to the above singlet pathway up to the singlet intermediate, which now dissociates endothermically without barrier to give the products. The second channel is the direct dissociation of the triplet intermediate, and is open only when an enough excess energy to surmount a triplet transition state is provided. The product energy distribution is also discussed based on the structures of transition states. © 1998 American Institute of Physics. [S0021-9606(98)00603-5]

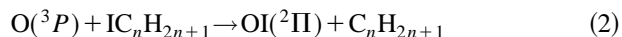
## I. INTRODUCTION

Recently, a number of experiments<sup>1-5</sup> have investigated the reactions of oxygen atoms with alkyl iodides. One of the principal reasons for interest in these systems is that one of the reactions that ensue following the collision of the two species is spin forbidden. Specifically, it has been observed that upon collision the following reaction occurs:



in which the reaction begins upon a triplet potential energy surface and produces products in the singlet state. The work of Leone and co-workers<sup>1,3</sup> is concerned primarily with the formation of these products, and examines the vibrational energy distribution in the nascent  $HOI$  molecules. Their experiments show that the  $HOI$  product formed in collisions of  $O(^3P)$  with alkyl iodides is vibrationally hot; the  $OH$  stretch is significantly excited.

A spin-allowed channel is also observed experimentally. The reaction



is studied by the experiments of Grice and co-workers.<sup>2,4,5</sup> Wang *et al.*<sup>2</sup> observe that in the case of oxygen colliding with ethyl iodide, the  $HOI$  product is distributed isotropically in the center of mass frame when the experiment is performed with a low relative translational energy and that the angular distribution becomes more anisotropic, with forward and backward peaking, as the collisional energy is increased. They report that the spin-forbidden process competes effectively with the spin-allowed chemical reaction. The spin-allowed channel is typically favored over the spin-forbidden channel. In particular, branching ratios varied from 1.6 to 3 in favor of  $OI$  and  $C_nH_{2n+1}$  for several systems studied with  $O$  atoms seeded in helium buffer gas and an energy of col-

lision of approximately 12 kcal/mol. Those collision experiments that are concerned in particular with ethyl iodide ( $C_2H_5I$ )<sup>2,4</sup> observe an angular distribution for  $OI$  products which is mildly forward and backward peaked at a low energy of collision and is sharply backward peaked at higher energies. The relative yield of  $OI$  increases as this backward peak appears. Wang *et al.*'s interpretation suggests that  $OI$  products are formed by two pathways, one of which is open at low impact energies and the other which opens at higher energies with a threshold of 8.6 kcal/mol.

In order to elucidate the mechanisms of the competing reactions in these systems, we have undertaken the investigation of the singlet and triplet potential energy surfaces involved in the reaction of  $O(^3P)$  with  $C_2H_5I$  by means of *ab initio* electronic structure calculations. Ethyl iodide is chosen as it is one of the smallest systems for which the formation of the  $HOI$  product is observed to occur.<sup>1</sup> After reviewing the method of computation in Sec. II, we discuss the geometry optimization at the B3LYP level in Sec. III. Section IV shows the results of high-level single-point calculations of the energy at the optimized geometries. The evaluation of the spin-orbit interaction in the presence of the iodine atom is presented in Sec. V, and Sec. VI provides a discussion of the accuracy of the calculations. Section VII deals with an improved optimization of the minimum on the singlet/triplet seam of crossing. Section VIII presents the final potential energy profile and the interpretation of the experiments for the  $O(^3P) + C_2H_5I$  reaction and conclusions.

## II. COMPUTATIONAL METHODS

All minima and transition states on the singlet and triplet potential surfaces of the  $C_2H_5I + O$  system were optimized using the B3LYP hybrid density functional method<sup>6</sup> and the 6-311 G(*d,p*) basis set, as specified in the G2M method.<sup>7</sup> As

no 6-311 G(*d,p*) basis is defined for the iodine atom, a basis set of valence triple-zeta+*d* polarization quality<sup>8</sup> associated with the relativistic MEFIT (multi-electron fit) effective core potential (ECP) of Bergner *et al.*<sup>9</sup> was used. The combined basis set, called basis set I, should be comparable to 6-311 G(*d,p*) for light atoms, and is used throughout the paper unless mentioned otherwise. The GAUSSIAN 94 package<sup>10</sup> was used to find all optima. Our own program has determined the minimum on the seam of crossing between the singlet and triplet potential energy surfaces (MSX).<sup>11</sup>

G2M<sup>7</sup> calculations were performed for better energetics at the B3LYP/I optimized geometries. A G2M(RCC,MP2) calculation was carried out, followed by a more computationally intensive G2M(RCC) calculation. These G2M computations implement the zero-point energies (ZPEs) calculated at the B3LYP/I level. The G2M(RCC,MP2) calculation entailed an RCCSD(T) (restricted coupled cluster singles and doubles with perturbation for triples) calculation of the energy followed by MP2 (Møller–Plessett second order) calculations to correct for larger basis sets. The large (4*s4p* CGTOs (contracted Gaussian-type orbitals) +3*df* polarization functions) iodine basis set developed for G2 calculations<sup>12</sup> with the 6-311G(3*df,2p*) basis set for lighter atoms (together called basis set II) was used for the basis set correction:  $\Delta E(+3df2p) = E(\text{MP2/II}) - E(\text{MP2/I})$ . Thus, one calculates the G2M(RCC,MP2) energy as

$$G2M(\text{RCC,MP2}) = E[\text{RCCSD(T)/I}] + \Delta E(+3df2p) \\ + \text{ZPE}(\text{B3LYP/I}) + \text{HLC},$$

where HLC is the higher level correction  $-0.525n_\beta - 0.525n_\alpha - 0.19n_\alpha$  in mhartree.<sup>7</sup> The G2M(RCC) calculation incorporates various corrections terms at the MP4 level. Specifically, the energy is calculated at the PMP4 level using basis set I, and additive basis set corrections are determined with PMP4 calculations with separate computations for the contribution of diffuse functions [a 6-311+G(*d,p*) basis set, using diffuse functions for the iodine atom determined for G2 methods,<sup>12</sup> to be referred to as basis set III] and for polarization functions [a 6-311G(2*df,p*) basis, with iodine G2 polarization functions used, referred to as basis set IV]. The scheme also employs a correction provided by RCCSD(T) and an MP2 correction using basis sets I and II. The total G2M(RCC) energy is given by

$$G2M(\text{RCC}) = E_{\text{bas}} + \Delta E(+) + \Delta E(2df) \\ + \Delta E(\text{RCC}) + \Delta' + \text{ZPE}(\text{B3LYP/I}) + \text{HLC},$$

where  $E_{\text{bas}} = E(\text{PMP4/I})$ ,  $\Delta E(+) = E(\text{PMP4/III}) - E_{\text{bas}}$ ,  $\Delta E(2df) = E(\text{PMP4/IV}) - E_{\text{bas}}$ ,  $\Delta' = E(\text{MP2/II}) - E(\text{MP2/III}) - E(\text{MP2/IV}) + E(\text{MP2/I})$ ,  $\Delta E(\text{RCC}) = E[\text{RCCSD(T)/I}] - E_{\text{bas}}$ ,  $\text{HLC} = 5.7 \ln_\beta - 0.19n_\alpha$  millihartree.

Corrections for spin-orbit effects arising from the presence of the iodine atom were computed using the GAMESS package. Section V describes these calculations in more detail.

Although there are several degenerate electronic states in the  $O(^3P)$  and  $O(^1D)$  reactants, as will be found later, the reaction pathway goes through very nonplanar  $C_1$  structures

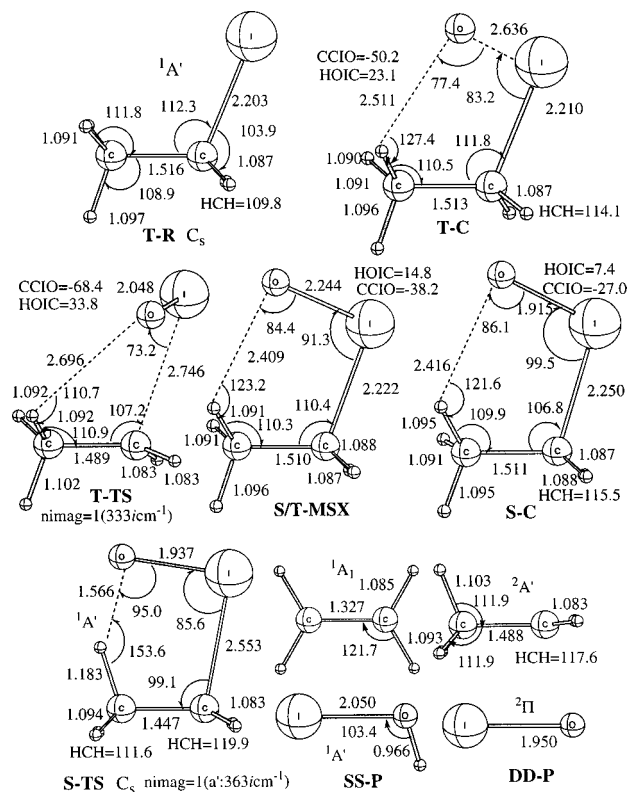


FIG. 1. B3LYP/I-optimized structures (in Å and deg) of reactants, intermediates, and transition states and the minimum of the singlet–triplet seam of crossing for the  $C_2H_5I + O$  system.

and therefore the reaction is expected to proceed on the lowest energy potential surface, without any symmetry constraint. Thus, we will consider only the lowest singlet and triplet states throughout the paper.

### III. THE B3LYP POTENTIAL ENERGY SURFACE

The structures of all the intermediates and transition states as well as reactants and products optimized in both the triplet and the singlet manifolds with the B3LYP/I method are shown in Fig. 1. Included also in Fig. 1 is the minimum of seam of crossing between the singlet and the triplet. The energies of the relevant species are shown in Table I, and the potential energy profile is displayed in Fig. 2 with the B3LYP/I energies in regular type. All the B3LYP/I energies (except for the MSX) presented include the zero-point energy (ZPE) correction calculated at the B3LYP/I level and are relative to the  $O(^3P)$  and  $C_2H_5I$  reactants, **T-R**.

Our computations found minima on both the singlet and triplet potential energy surfaces, referred to as **T-C** and **S-C**, respectively, with energies of  $-6.4$  and  $-15.4$  kcal/mol. The triplet minimum **T-C** corresponds to van der Waals complexes between the reactants,  $O(^3P)$  and  $C_2H_5I$ . The short  $I \cdots O$  distance of  $2.6$  Å indicates a moderate interaction between I and O, and the  $H \cdots O$  distance of  $2.51$  Å also suggests some attractive interaction between them. One of the oxygen lone pairs interacts donatively with one of the hydrogen atoms of  $CH_3$  and the iodine lone pair donatively interacts with the half-occupied *p* orbital of oxygen, as illustrated in Fig. 3(A). The singlet minimum **S-C** is a hypervalent mol-

TABLE I. B3LYP/I, G2M(RCC,MP2), and G2M(RCC) energies (in kcal/mol) of B3LYP/I optimized structures, relative to the  $O(^3P) + C_2H_5I$  reactants. Some contributions to the G2M energies are also displayed, as well as energies corrected for spin-orbit effects.

Structure	Label	ZPE	B3LYP/I +ZEP	RCCSD(T)/I +ZPE	E(PMP4/I) +ZPE	G2M (RCC,MP2)	G2M (RCC)	G2M (RCC/MP2) +SO	G2M (RCC) +SO
$O(^3P) + C_2H_5I$	<b>T-R</b>	41.0	0	0	0	0	0	0	0
Triplet complex	<b>T-C</b>	41.5	-6.4	2.7	3.9	-6.8	-6.7	-6.8	-6.7
Triplet TS	<b>T-TS</b>	39.8	12.2	33.0	30.9	24.1	27.1	22.6	25.6
MSX (triplet)	<b>S/T-MSX</b>	...	-1.6 <sup>a</sup>	12.4 <sup>a</sup>	13.1 <sup>a</sup>	0.4 <sup>a</sup>	2.7 <sup>a</sup>	1.0 <sup>a</sup>	2.8 <sup>a</sup>
MSX (singlet)	<b>S/T-MSX</b>	...	-1.6 <sup>a</sup>	8.5 <sup>a</sup>	11.2 <sup>a</sup>	-15.9 <sup>a</sup>	-13.0 <sup>a</sup>	-15.3 <sup>a</sup>	-13.0 <sup>a</sup>
Singlet complex	<b>S-C</b>	41.9	-15.4	-3.4	-4.0	-36.6	-31.7	-36.1	-31.8
Singlet TS	<b>S-TS</b>	40.3	-14.1	0.4	-1.0	-30.2	-25.6	-29.8	-25.7
HOI + $C_2H_4$	<b>SS-P</b>	39.7	-52.3	-41.8	-42.2	-59.6	-57.4	-60.0	-57.8
OI + $C_2H_5$	<b>DD-P</b>	37.9	6.2	21.3	22.4	10.3	10.3	7.6	8.0

<sup>a</sup>Energies without the inclusion of zero-point energies.

ecule  $C_2H_5IO$ . The O-I distance of 1.92 Å is even shorter than in OI, and the I-C distance of 2.25 Å is only slightly longer than 2.20 Å in  $C_2H_5I$ . One of the iodine lone pairs forms a donative  $\sigma$  bond with the oxygen vacant  $p$  orbital, with one of the oxygen lone pairs interacting donatively with one of the hydrogen atoms of  $CH_3$ , as illustrated in Fig. 3(B). The IO bond is very ionic, with  $O^-I^+$  polarization, as is also illustrated with the Mulliken charges in Fig. 3(B).

The minimum on the singlet surface **S-C** has been found to connect directly to the doublet OI and doublet  $C_2H_5$  products, **DD-P**, with no intervening reverse barrier. On the triplet surface, there is a barrier between **T-C** and **DD-P**; the transition state for formation of the OI product on the triplet surface, **T-TS**, appears at an energy of 12.2 kcal/mol, placing it 18.6 kcal/mol above the minimum **T-C** and 6.0 kcal/mol above the products **DD-P**. The I-O internuclear separation in **T-TS** has decreased to 2.05 Å, much closer to 1.95 Å in the OI product than to 2.64 Å in **T-C**, and the C-I internuclear separation of 2.75 Å in **T-TS** is approximately 24% longer than in **T-C**, both pointing to a late transition state for the formation of OI product.

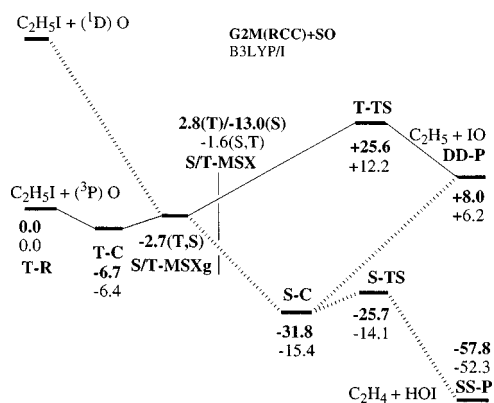


FIG. 2. The singlet and triplet potential energy profile of the  $C_2H_5I + O$  system, scaled to the most rigorous G2M(RCC)+SO results. The triplet surface is represented by dashed lines, and the singlet surface by solid lines. The G2M(RCC)+SO and B3LYP/I energies (in kcal/mol, including ZPE, except for the MSX's) of the optimized structures are in bold and regular type, respectively.

On the singlet surface, a five-membered ring transition state **S-TS** has been found to connect the minimum **S-C** to the singlet HOI + singlet ethylene products, **SS-P**. The barrier lies 1.3 kcal/mol above the minimum and 38.2 kcal/mol above the products. At the transition state **S-TS** the C-H and the C-I bonds to be broken are 10%–14% stretched, while the O-H bond to be formed is still 60% longer than in the product, demonstrating a very early nature of a transition state typical of highly exothermic reactions. This long O-H distance at the singlet transition state will be discussed again later in connection with the product vibrational excitation. A transition state similar to **S-TS** has been quoted by Loomis *et al.*<sup>1</sup> The OI and  $C_2H_5$  products, **DD-P**, and the HOI and  $C_2H_4$  products, **SS-P**, are at 6.2 and -52.3 kcal/mol, respectively, relative to the reactants. The optimized HO bond distance of 0.966 Å for HOI agrees well with the experimental value of 0.964 Å by Klaasen *et al.*<sup>3</sup>

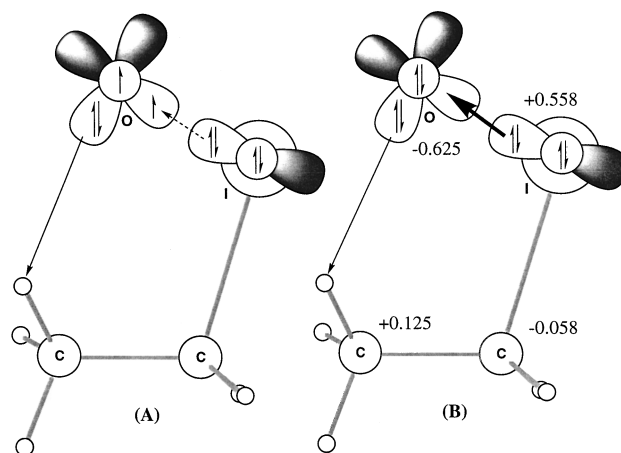


FIG. 3. The electronic structures of triplet and singlet complexes. (A) The triplet minimum **T-C** is a van der Waals complex, stabilized by the donative interaction of lone pair electrons on the iodine atom to a singly occupied  $p$  orbital on the oxygen atom, and the interaction of a lone pair in a  $p$  orbital on oxygen with the hydrogen atom. (B) The singlet minimum **S-C** is a hypervalent molecule  $C_2H_5IO$ , stabilized by donation from a lone pair in a  $p$  orbital on iodine to a vacant  $p$  orbital on oxygen, and an interaction between a lone pair on oxygen and the hydrogen atom. The Mulliken charges on I, O,  $CH_2$ , and  $CH_3$  groups at the B3LYP/I level are shown.

The minimum of the seam of crossing between the triplet and singlet potential surfaces, **S/T-MSX**, has been located between the two minimum structures, **T-C** and **S-C**. It lies energetically (without ZPE) at  $-1.6$  kcal/mol relative to the reactants, and  $5.4$  and  $14.8$  kcal/mol, respectively, above the two minima **T-C** and **S-C** connected by this MSX. There is no barrier between the MSX and the two minima. The structure of this MSX is closer to **T-C** than to **S-C**, reflecting the energetics.

#### IV. G2M SINGLE POINT ENERGY CALCULATIONS

For better energetics, G2M(RCC,MP2) and more rigorous G2M(RCC) computations were performed at the B3LYP/I optimized geometries. Table I summarizes the results and compares with the B3LYP/I energies. Although the qualitative picture of the potential energy profile remains unchanged upon going from B3LYP/I to small basis coupled cluster and MP4 to G2M methods, the details of the energetics change substantially.

For instance the RCCSD(T)/I and MP4/I calculations place the triplet structure **T-C**, which was a minimum at the B3LYP/II level,  $2.7$  and  $3.9$  kcal/mol above the  $C_2H_5I$  and  $O(^3P)$  reactants. The RCCSD(T)/I and MP4/I relative energies are about  $10$  kcal/mol higher for the  $HOI + C_2H_4$  products than the B3LYP/I results and about  $15$  kcal/mol higher for the  $OI + C_2H_5$  products. However, the G2M(RCC,MP2) and G2M(RCC) results are much closer to the B3LYP/I results than to the RCCSD(T)/I. With the G2M methods, the triplet complex **T-C** is lower than the  $C_2H_5I$  and  $O(^3P)$  reactants. The G2M energies of both  $HOI + C_2H_4$  and  $OI + C_2H_5$  products are similar to the B3LYP/I energies. The G2M(RCC,MP2) and G2M(RCC) methods, as discussed in Sec. II, start with the RCCSD(T)/I method and add the correction for the basis sets evaluated at the MP2 and MP4 levels, respectively. In the present system, the corrections for polarization and diffuse basis functions are found to be the most important terms affecting the energetics. Apparently, the B3LYP method with a small basis set seems to reproduce the highly correlated results with a larger basis set.

However, there are several important differences between the B3LYP/I and G2M results. For instance, the energy of the triplet transition state **T-TS**, as well as that of the triplet products  $OI + C_2H_5$ , is predicted to be higher in the G2M methods than in the B3LYP/I method. The B3LYP/I method seems to be underestimating the barrier height for the forward reaction from **T-C** as well as for the reverse reaction from  $OI + C_2H_5$ . The singlet complex **S-C**, as well as the singlet transition state **S-TS**, is much more stable in the G2M methods than in the B3LYP/I method. The binding energy of the hypervalent intermediate **S-C** seems to be substantially underestimated by the B3LYP/I method.

#### V. SPIN-ORBIT CORRECTIONS TO THE ENERGY

Spin-orbit corrections (SO) to the energy have been calculated for all structures in Fig. 1 that contain an iodine atom. The spin-orbit interaction energy was calculated with complete active space self-consistent field (CASSCF) singlet

TABLE II. Shifts in the ground state energies of iodine containing species resulting from CASSCF/I spin-orbit coupling calculations.

Structure	Label	cm <sup>-1</sup>	kcal/mol
I atom		-2534	-7.2
$C_2H_5I$	<b>T-R</b>	-4	-0.0
Triplet complex	<b>T-C</b>	-1	-0.0
Triplet transition state	<b>T-TS</b>	-537	-1.5
MSX (triplet)	<b>S/T MSX</b>	15	0.0
MSX (singlet)	<b>S/T MSX</b>	-15	-0.0
Singlet complex	<b>S-C</b>	-15	-0.0
Singlet transition state	<b>S-TS</b>	-51	-0.1
HOI	<b>SS-P</b>	-141	-0.4
OI	<b>DD-P</b>	-805	-2.3

and triplet wave functions as a basis, using the one-electron effective spin-orbit Hamiltonian implemented in the GAMESS electronic structure package by Koseki *et al.*<sup>13</sup> In these calculations, although the effective nuclear charge  $Z_{\text{eff}}$  of Koseki is used for the carbon, hydrogen, and oxygen atoms, the contribution of the heavy iodine atom dominates. The effective nuclear charge  $Z_{\text{eff}}$  of the iodine atom was chosen to be 6712, so that a  $(7e/4o)$  CASSCF+ the effective spin-orbit calculation with the basis set I for the iodine atom reproduced the experimentally found  $^2P_{3/2} - ^2P_{1/2}$  splitting of  $21.7$  kcal/mol.<sup>14</sup> For the MSX, the singlet and triplet minima, and the transition states, we used an  $(8e/6o)$  active space, consisting of the three  $p$  orbitals on oxygen, the two nonbonding  $p$  orbitals on iodine and the  $C-I \sigma^*$  antibonding orbital. The ethyl iodide reactant calculations use a  $(4e/3o)$  active space consisting of the two iodine nonbonding  $p$  orbitals and the  $C-I \sigma^*$  orbital, while the HOI product is treated with a  $(6e/5o)$  active space including the one O and two I nonbonding  $p$  orbitals and the  $O-I \sigma$  and  $\sigma^*$  orbitals. The  $(7e/6o)$  active space for the OI product consists of the two iodine and two oxygen nonbonding  $p$  orbitals and the  $O-I \sigma$  and  $\sigma^*$  orbitals, where the spin-orbit interaction splits the  $^2\Pi$  state to the  $^2\Pi_{1/2}$  and  $^2\Pi_{3/2}$  states. The spin-orbit corrections to the energy obtained in these calculations are summarized in Table II, and the revised energetics is presented in the final columns of Table I.

The spin-orbit corrections to the energies of the species involved in the reaction are in general small. The largest correction is for the OI product, which is calculated to be  $-2.3$  kcal/mol, to be compared with the experimental value of  $-3.0$  kcal/mol.<sup>15</sup> The triplet transition state **T-TS**, which is close in structure to  $OI + C_2H_5$ , has the next largest correction of  $-1.5$  kcal/mol. In other intermediates and transition states, the spin-orbit interaction is very much "quenched" and made negligibly small by delocalization of spin from the I atom.

The spin-orbit coupling calculation at the MSX is of particular interest, as it will determine the transition probability from the triplet to the singlet potential energy surface. The CASSCF calculations gives the spin-orbit coupling element between the two states to be  $202 \text{ cm}^{-1}$  or  $0.58$  kcal/mol, a substantial coupling element. Since the singlet and triplet CASSCF energies at the B3LYP/I-determined seam of

TABLE III. Energies (in kcal/mol, at 0 K) and enthalpies (in kcal/mol, at 298 K and 1 atm, in italic) of various reactions computed at various levels of theory and compared with experiments.

No.	Reaction	B3LYP/I +ZPE+SO	G2M(RCC,MP2) +SO	G2M(RCC) +SO	Experimental
3	OI→O+I	42.0	46.8	45.7	53 <sup>a</sup> , 42 <sup>b</sup>
4	HOI→OH+I	36.0	46.3	43.8	56 <sup>c,d</sup> , 43 <sup>e</sup>
5	HOI→OI+H	93.4	101.3	100.01	114 <sup>d</sup> , 94.2–95.2 <sup>e</sup>
6	C <sub>2</sub> H <sub>5</sub> I→C <sub>2</sub> H <sub>5</sub> +I	45.7	54.2	53.5	53.1 <sup>f</sup>
7	C <sub>2</sub> H <sub>5</sub> →C <sub>2</sub> H <sub>4</sub> +H	36.6	33.4	33.1	38.8 <sup>f</sup>
1	C <sub>2</sub> H <sub>5</sub> I+O→HOI+C <sub>2</sub> H <sub>4</sub>	-51.0	-58.6	-56.7	-53, -66
2	C <sub>2</sub> H <sub>5</sub> I+O→OI+C <sub>2</sub> H <sub>5</sub>	3.9	7.6	8.0	0.1

<sup>a</sup>Reference 16(b).<sup>b</sup>Reference 16(e).<sup>c</sup>Reference 16(f).<sup>d</sup>Reference 16(g).<sup>e</sup>Reference 16(c).<sup>f</sup>Reference 16(a).

crossing are different by 11.9 kcal/mol, the change of the energies of these CASSCF states due to the spin-orbit interaction is only  $\pm 15 \text{ cm}^{-1}$ , as shown in Table II. The determination of MSX with more reliable energetics will be discussed again in Sec. VIII.

## VI. BENCHMARK CALCULATIONS ON RELEVANT MOLECULES

Here we will compare theoretical values with experimental values and estimates<sup>16</sup> for the energies (or enthalpies) of reaction (1) and (2), as well as various related reactions that are used to derive the energies of (1) and (2). Table III summarizes the results.

The dissociation energy of OI, reaction (3), does not seem to be well established experimentally. Most recently, Radlein *et al.*<sup>16(b)</sup> give  $53 \pm 3$  kcal/mol (also estimated by Ruscic<sup>16(c)</sup> to be  $50 \pm 5$  kcal/mol). However, Huber and Herzberg<sup>16(d)</sup> do not quote this number, but consider an earlier number of 56 kcal/mol from flame photochemistry to be too high (too close to the OBr dissociation energy of 55 kcal/mol). They refer to the value of 42 kcal/mol obtained from the extrapolation of vibrational levels.<sup>16(e)</sup> The G2M(RCC) value of 46 kcal/mol is in reasonable agreement with 46 kcal/mol but is too low by 7 kcal/mol compared to 53 kcal/mol. G2 and quadratic CI computations of McGrath and Rowland<sup>17</sup> gave 51–52 kcal/mol for this energy. However, we suspect that this number is unreliable, as the use of an ‘unrestricted’ method like G2 would result in a heavily spin-contaminated wave function. The energy of the HOI→OH+I reaction, reaction (4), has two very different sets of experimental values, 56 kcal/mol of Gelles<sup>17(f)</sup> and 56.3 kcal/mol estimated by Maguin *et al.*<sup>17(g)</sup> vs 43 kcal/mol estimated by Ruscic *et al.*<sup>17(c)</sup> The present G2M(RCC) value of 44 kcal/mol is closer to and supports the latter result. The most recent experimental estimate of the O–H dissociation energy of HOI reaction (5), 94.2–95.2 kcal/mol by Ruscic *et al.*,<sup>17(c)</sup> is smaller than an earlier estimate of 114 kcal/mol by Maguin *et al.*<sup>17(e)</sup> and agrees better with the present G2(RCC) value of 100 kcal/mol. The combination of energies of reactions (3)–(4)+(5) should give the dissociation

energy of OH, to be compared as an internal test with the experimental value of 102.3 kcal/mol.<sup>16(b)</sup> The use of 43 kcal/mol for (4) and 95 kcal/mol for (5) with the two values, 53 and 42 kcal/mol, for (1) result in 105 and 94 kcal/mol, respectively, with an error of 3 and –8 kcal/mol. One should note that the bond dissociation energy of OH is well reproduced by the G2M(RCC) calculation, which gives 102 kcal/mol. The reaction  $C_2H_5I \rightarrow C_2H_5 + I$ , reaction (6), is found to have an enthalpy of 54 kcal/mol at the G2(RCC) level, which agrees well with the experimental value of 53.1 extracted from the tables of Rosenstock *et al.*<sup>16(a)</sup>

We will now discuss the energies of the two reactions of primary interest. The enthalpy of spin-forbidden reaction (1):  $C_2H_5I + O \rightarrow C_2H_4 + HOI$  can be estimated from the experimental values of reactions (4), (6), and (7) in Table III and the bond dissociation energy of 102.3 kcal/mol for OH<sup>16(a)</sup> to be –53 kcal/mol, if we adopt the preferred H–OI dissociation energy of 43 kcal/mol. The calculated G2M(RCC) value of –57 kcal/mol is in reasonable agreement with the experiment, with an error of 4 kcal/mol. One may also compare this with –59.2 kcal/mol, a G2(MP2) result of Marshall *et al.* quoted by Loomis *et al.*<sup>1</sup> One should note that, if a higher value of 56 kcal/mol is used for the experimental H–OI dissociation energy, the energy of reaction (1) would be –66 kcal/mol.

The experimental energy of the spin-allowed reaction (2):  $C_2H_5I + O \rightarrow C_2H_5 + OI$  can be obtained from those of the reactions (3) and (6) in Table III to be 0.1 kcal/mol (thermo-neutral) if 53 kcal/mol is adopted for the experimental OI bond dissociation energy, or +11 kcal/mol (endothermic) if 42 kcal/mol is used. The calculated G2M(RCC) energy is +8 kcal/mol, too endothermic if 53 kcal/mol is used for the experimental OI dissociation energy. The computed error in the energy of this reaction and the dissociation energy might be attributed to a computed energy of OI which is too high relative to the reactants. The error might be attenuated by the use of larger basis sets to treat the polarization of electrons in iodine or a better geometry optimization of OI.

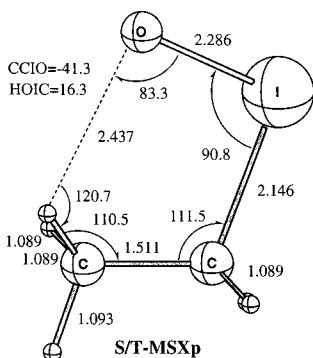


FIG. 4. The structure (in Å and deg) of the minimum of the singlet–triplet seam of crossing, optimized at the MP2/IV level.

## VII. ADDITIONAL COMPUTATIONS OF THE MINIMUM OF THE SEAM OF CROSSING

The computations find that the minimum of the seam of singlet–triplet crossing, **S/T-MSX**, as located using B3LYP/I geometry optimization in Fig. 1, is not a point at which the singlet and triplet surfaces are degenerate at the G2M(RCC) level. Actually at this geometry the G2M(RCC) singlet state is found to be more stable by 15.7 kcal/mol than the triplet, as shown in Table I. The relative energetics in Fig. 2 suggests that the true minimum of the seam of crossing at the G2M level should geometrically lie closer to the triplet complex **T-C** than does the present **S/T-MSX**. Reoptimization of the MSX at the G2M(RCC) or G2M(RCC,MP2) level, however, is impossible because of the lack of analytical gradient at these levels.

The analysis of the individual correction terms in the G2M(RCC) and G2M(RCC,MP2) energies indicates that several different terms contribute to this singlet–triplet energy difference and that the largest though not dominant (30%) contribution comes from the correction for the polarization functions evaluated at the MP4 or MP2 level. Therefore, we have reoptimized the MSX at the MP2/IV level, where the basis set IV, as explained in Sec. II, consists of  $4s4p$  CGTOs +  $3df$  polarization function for iodine and  $6-311G(2df,p)$  for the other atoms. The MP2/IV reoptimized MSX, called **S/T-MSXp**, is shown in Fig. 4.

The structure of **S/T-MSXp** is indeed earlier in the reaction coordinate and lies between those of **T-C** and **S/T-MSX**. The  $O\cdots H$  distance in **S/T-MSXp** is 0.07 Å shorter than in **T-C** but 0.03 Å longer than in **S/T-MSX** and the  $O\cdots I$  distance is 0.35 Å shorter than in **T-C** but 0.04 Å longer than in **S/T-MSX**. The G2M(RCC) energies (relative to the reactant) at **S/T-MSXp** are +0.6 kcal/mol for the triplet and –9.0 for the singlet, compared to +2.7 and –13.0 kcal/mol, respectively, at **S/T-MSX**. Although the singlet–triplet energy difference is reduced from 15.7 to 11.7 kcal/mol, **S/T-MSXp** is still far from the true MSX at the G2M(RCC) level. Assuming that both the singlet and triplet change their energies linearly with the geometry change,  $R(S/T-MSXp) - R(S/T-MSX)$ , which has taken place from **S/T-MSX** to **S/T-MSXp**, a one-dimensional extrapolation predicts that the geometry of the true G2M(RCC)

**MSX**, **S/T-MSXg** lies at  $R(S/T-MSXg) = R(S/T-MSXp) + 1.57*[R(S/T-MSXp) - R(S/T-MSX)]$ , and the degenerate G2M(RCC) energy both for the singlet and the triplet at this true MSX, **S/T-MSXg**, would be –2.7 kcal/mol. Although this extrapolation scheme may be oversimplified, the important finding is that the energy at this G2M(RCC) crossing is slightly below the energy of the reactants.

A CASSCF spin–orbit calculation performed at the MP2IV-optimized **S/T-MSXp** gives a singlet–triplet coupling matrix element of  $224\text{ cm}^{-1}$ , which is a little larger than the value of  $202\text{ cm}^{-1}$  at the B3LYP/I-optimized **S/T-MSX**. The spin–orbit coupling element at the G2M-extrapolated **S/T-MSXg** would be  $260\text{ cm}^{-1}$ , if the linear extrapolation done above is also allowed here.

## VIII. THE FINAL POTENTIAL ENERGY PROFILE AND THE INTERPRETATION OF THE EXPERIMENTS FOR THE $O(^3P) + C_2H_5I$ REACTION

The final overall potential energy profile at the G2M(RCC)+SO level, including the extrapolated energies at **S/T-MSXg**, is shown in Fig. 2, with the energetics in bold character. We will discuss the mechanism of the  $O(^3P) + C_2H_5I$  reaction, using this potential energy profile.

At first we will discuss the spin-forbidden reaction (1), leading to the singlet products  $HOI + C_2H_4$ . Figure 2 indicates that this reaction has to take place via the initial triplet complex **T-C**, the intersystem-crossing (isc) from the overall triplet potential surface of the reactants to the singlet at the singlet–triplet MSX **S/T-MSXg**, the singlet intermediate **S-C**, and the singlet five-membered ring transition state **S-TS**. The energetics indicates that the highest point in the energy in this channel is at **S/T-MSXg**, which is below the energy of the reactants. Thus this channel is expected to be open at any collision energy, and is the only open reactive channel at lower energies. Experimentally, this channel has been observed at a low collision energy of 3.8 kcal/mol.<sup>2</sup> At a low energy, the system will spend more time in the vicinity of the triplet complex **T-C**, before reaching **S/T-MSXg** and making isc with a small probability. We expect that the scattering to produce HOI will be isotropic at a low energy and that as the collision energy increases, and the lifetime of the triplet complex decreases, the scattering will become more anisotropic. This is what is found experimentally for the reaction (1).<sup>2</sup>

The singlet transition state **S-TS** leading to HOI product, as shown in Fig. 1, is the transition state for intramolecular  $\beta$ -H abstraction by the leaving OI group.<sup>3</sup> The extraction of H from the carbon atom  $\beta$  to the iodine atom is consonant with the mechanism proposed by Loomis *et al.*<sup>1</sup> The **S-TS** has an O–H bond distance of 1.57 Å, which is much longer than the O–H distance of 0.97 Å in the HOI product. If this large O–H extension or a substantial part of it is assumed to remain in the product, one would expect a large OH vibrational excitation in the nascent HOI product. Experimentally, this is exactly what is observed.<sup>1,3</sup> The geometry of **S-TS** also suggests that in the HOI product, the bending vibration will be modestly excited, while the OI stretch would not be.

A large potential energy release from a relatively early transition state suggests a large translational energy as well.

Now we will discuss the spin-allowed reaction (2), leading to the radical-radical products  $OI(^2\Pi) + C_2H_5$ . Figure 2 indicates that there are two pathways leading to these products. One is the singlet pathway, following the same route with the reaction (1), via the initial triplet complex **T-C**, the intersystem-crossing (isc) from the overall triplet potential surface of the reactants to the singlet at the singlet-triplet **MSX S/T-MSXg** and the singlet intermediate **S-C**, from where, deviating from the reaction (2), the system dissociates endoergically without reverse barrier to give the radical-radical products. This channel should become open as soon as the collision energy can supply an enough energy to reach  $OI(^2\Pi) + C_2H_5$ . As discussed in Sec. VI, the reaction (2) is supposed to be nearly thermoneutral (if one set of the experimental  $OI$  dissociation energy is used), and thus this channel should be open at very low collision energies. Since this channel takes place via the **T-C** complex, like the reaction channel (1), the scattering is expected to be isotropic at a low energy. This agrees with the experimental finding.<sup>2</sup>

Figure 2 indicates that at higher energy a new channel should open for reaction (2). This is the spin-allowed channel all in the triplet manifold via the transition state **T-TS**. Since this is a direct channel, the scattering is expected to be backward. Experimentally, as the impact energy increases, the scattering becomes more anisotropic, in particular backward.<sup>2</sup> Wang *et al.*<sup>2</sup> note that backward scattering appears only at the initial center of mass translational energy of about 8.6 kcal/mol, and suggest that a new channel opens up at this energy, which corresponds to the system having enough energy to surmount a barrier to  $OI$  formation on the triplet energy surface. As the collision energy increases, this direct triplet channel should be come dominant over the singlet channel which involves inefficient triplet/singlet transition. The geometry of the transition state **T-TS** suggests that the  $IO$  product is likely to be rotationally excited but vibrationally cold and the ethyl product may be slightly excited vibrationally. The present G2M(RCC) calculation finds the energy of the **T-TS** to be 25.6 kcal/mol above the reactants. This is too high in comparison with the experiment. As discussed above (Table III), the products **DD-P** of the reaction (2) are calculated to be 8.0 kcal/mol above the reactants, versus the one of the experimental estimates of 0.1 kcal/mol. Considering that **T-TS** is a late transition state, it would be justifiable to reduce its energy by the error at the products, 7.9 kcal/mol, which will give the adjusted energy of **T-TS** to be 17.7 kcal/mol, which is still too large by 9.1 kcal/mol, in comparison with the experiment. To justify this error in part, one may argue that the experimental initial translational energy should have a distribution around the peak at 8.6 kcal/mol, and the threshold of the reaction may actually be somewhat higher than the peak energy.

If the reaction is carried out by the collision of  $O(^1D)$ , instead of  $O(^3P)$ , with  $CH_3CH_2I$ , the potential energy profile in Fig. 2 suggests that the direct singlet channel producing  $HOI + C_2H_4$  would be dominant at all the collision energies, with a minor contribution of the singlet channel giving

$IO + C_2H_5$  product as well as other channels, such as direct hydrogen abstraction by  $O(^1D)$ , not explored in the present study.

It has been recently learned that a new beam experiment has been performed by Alagia *et al.* for the reaction of the smallest analog,  $CH_3I$ , with both  $O(^3P)$  and  $O(^1D)$ .<sup>18</sup> The major difference of these reactions of  $CH_3I$  from those of  $CH_3CH_2I$  would be the lack of the  $\beta$ -hydrogen abstraction channel, **S-TS** and **SS-P**. Otherwise the potential energy profile would be similar, with some minor changes in the energetics. Thus,  $O(^1D)$  will produce  $IO + CH_3$  via the direct singlet channel, with some other possible minor channels not explored here.  $O(^3P)$  will produce  $IO + CH_3$  via isc and the singlet intermediate at lower collision energies and the same product via the direct triplet mechanism at higher energies.

In conclusion, the calculations presented here provide mechanisms for the formation of both spin-forbidden  $HOI$  and spin-allowed  $OI$  products.  $HOI$  is formed by a triplet to singlet intersystem crossing, followed by passage through a singlet transition state, which is accessible even at low impact energies. This is consonant with experiments which observe these products at low impact energies and which indicated that  $HOI$  is formed via abstraction of a hydrogen from the  $\beta$  carbon of ethyl iodide.  $OI$  may be formed by two pathways, one which again is accessible at low energies through the singlet pathway and the other which may only be observed if there is sufficient energy to surmount a barrier in the triplet state. Again this is consonant with recent experiments probing the reaction mechanism.

## ACKNOWLEDGMENTS

The authors would like to acknowledge Dr. Fred Strobel and James Breslin for discussions of scattering experiments and Dr. Max Holthausen for discussions of the computation of the electronic structure of halogen atoms. This work was in part supported by Grant No. F49620-95-1-0182 from the Air Force Office of Scientific Research.

<sup>1</sup>R. A. Loomis, J. J. Klaassen, J. Linder, P. G. Christopher, and S. R. Leone, *J. Chem. Phys.* **106**, 3934 (1996).

<sup>2</sup>J. J. Wang, D. J. Smith, and R. Grice, *J. Phys. Chem.* **100**, 13603 (1996).

<sup>3</sup>J. J. Klaassen, J. Linder, and S. R. Leone, *J. Chem. Phys.* **104**, 7403 (1996).

<sup>4</sup>J. J. Wang, D. J. Smith, and R. Grice, *J. Chem. Phys.* **100**, 6620 (1996).

<sup>5</sup>R. W. P. White, D. J. Smith, and R. Grice, *Chem. Phys. Lett.* **193**, 269 (1992).

<sup>6</sup>A. D. Becke, *J. Chem. Phys.* **98**, 5648 (1993); **96**, 2155 (1992).

<sup>7</sup>A. M. Mebel, K. Morokuma, and M. C. Lin, *J. Chem. Phys.* **103**, 7414 (1995).

<sup>8</sup>M. Dolg, Ph.D. dissertation, University of Stuttgart, 1990.

<sup>9</sup>A. Bergner, M. Dolg, W. Kuchle, H. Stoll, and H. Press, *Mol. Phys.* **80**, 1431 (1993).

<sup>10</sup>GAUSSIAN 94, Revision A. 1, M. J. Frisch, G. W. Trucks, H. B. Schlegel, P. M. W. Gill, B. G. Johnson, M. A. Orb, J. R. Chessman, T. Keith, G. A. Peterson, J. A. Montgomery, K. Raghavachari, M. A. Al-Laham, V. G. Zakrzewski, J. V. Ortiz, J. B. Foresman, J. Cioslowski, B. B. Stefanov, A. Nanayakkara, M. Challacombe, C. Y. Peng, P. Y. Ayala, W. Chen, M. W. Wong, J. L. Andres, E. S. Replogle, R. Gomperts, R. L. Martin, D. J. Fox, J. S. Binkley, D. J. Defrees, J. Baker, J. P. Stewart, M. Head-Gordon, C. Gonzalez, and J. A. Pople, Gaussian, Inc., Pittsburgh, PA, 1995.

<sup>11</sup>C. Qiang and K. Morokuma, *Chem. Phys. Lett.* **263**, 54 (1996).

- <sup>12</sup>M. N. Glukhovtsev, A. Pross, M. P. McGrath, and L. Radom, *J. Chem. Phys.* **103**, 1878 (1995).
- <sup>13</sup>S. Koseki, M. S. Gordon, M. W. Schmidt, and N. Matsunaga, *J. Phys. Chem.* **99**, 12764 (1995).
- <sup>14</sup>C. E. Moore, *Atomic Energy Levels* (USGPO, Washington, DC, 1971), Vols. II and III, NSRDS-NBS 35.
- <sup>15</sup>J. P. Bekooy, W. Leo Meerts, and A. Dynamus, *J. Mol. Spectrosc.* **102**, 320 (1983).
- <sup>16</sup>(a) H. M. Rosenstock, K. Draxl, B. W. Steiner, and J. T. Herron, *J. Chem. Phys. Ref. Data*, 6, Suppl. 1 (1977); (b) D. St. A. G. Radlein, J. C. Whitehead, and R. Grice, *Nature (London)* **253**, 37 (1985); (c) B. Ruscic and J. Berkowitz, *J. Chem. Phys.* **101**, 7795 (1994); (d) K. P. Huber and G. Herzberg, *Molecular Spectra and Molecular Structure*, (van Nostrand Reinhold, New York, 1979), Vol IV; (e) R. A. Durie and D. A. Ramsey, *Can. J. Chem.* **36**, 45 (1958); (f) E. Gelles, *Trans. Faraday Soc.* **47**, 1158 (1951); (g) F. Maguin, G. Laverdet, G. LeBras, and G. Poulet, *J. Phys. Chem.* **96**, 1775 (1992).
- <sup>17</sup>M. P. McGrath and F. S. Rowland, *J. Phys. Chem.* **100**, 4815 (1996).
- <sup>18</sup>M. Alagia, N. Balucani, L. Cartechini, P. Casavecchia, M. C. van Beek, and G. G. Volpi, presented at the 1997 Conference on the Dynamics of Molecular Collisions, Brainerd, MN, 20–25 July 1997 (unpublished).